HAL
open science

Parameterization of N2O5 reaction probabilities on the surface of particles containing ammonium, sulfate, and nitrate

J. M. Davis, P. V. Bhave, K. M. Foley

To cite this version:

J. M. Davis, P. V. Bhave, K. M. Foley. Parameterization of N2O5 reaction probabilities on the surface of particles containing ammonium, sulfate, and nitrate. Atmospheric Chemistry and Physics Discussions, 2007, 7 (6), pp.16119-16153. hal-00303176

HAL Id: hal-00303176

https://hal.science/hal-00303176v1

Submitted on 18 Jun 2008

HAL is a multi-disciplinary open access archive for the deposit and dissemination of scientific research documents, whether they are published or not. The documents may come from teaching and research institutions in France or abroad, or from public or private research centers.

L'archive ouverte pluridisciplinaire **HAL**, est destinée au dépôt et à la diffusion de documents scientifiques de niveau recherche, publiés ou non, émanant des établissements d'enseignement et de recherche français ou étrangers, des laboratoires publics ou privés.

Atmos. Chem. Phys. Discuss., 7, 16119–16153, 2007
www.atmos-chem-phys-discuss.net/7/16119/2007/
© Author(s) 2007. This work is licensed
under a Creative Commons License.

Atmospheric Chemistry and Physics Discussions

Parameterization of N_2O_5 reaction probabilities on the surface of particles containing ammonium, sulfate, and nitrate

J. M. Davis[1,*], P. V. Bhave[2], and K. M. Foley[2]

[1]Atmospheric Modeling Division, U.S. Environmental Protection Agency, Research Triangle Park, NC, USA
[2]Atmospheric Sciences Modeling Division, Air Resources Laboratory, National Oceanic and Atmospheric Administration, Research Triangle Park, NC, USA
[*]now at: North Carolina State University, Department of Marine, Earth, and Atmospheric Sciences, Raleigh, NC, USA

Received: 19 October 2007 – Accepted: 23 October 2007 – Published: 19 November 2007

Correspondence to: J. M. Davis (davisj@ncsu.edu)

Abstract

A comprehensive parameterization was developed for the heterogeneous reaction probability (γ) of N_2O_5 as a function of temperature, relative humidity, particle composition, and phase state, for use in advanced air quality models. The reaction probabilities on aqueous NH_4HSO_4, $(NH_4)_2SO_4$, and NH_4NO_3 were modeled statistically using data and uncertainty values compiled from seven different laboratory studies. A separate regression model was fit to laboratory data for dry NH_4HSO_4 and $(NH_4)_2SO_4$ particles, yielding lower γ values than the corresponding aqueous parameterizations. The regression equations reproduced 79% of the laboratory data within a factor of two and 53% within a factor of 1.25. A fixed value was selected for γ on ice-containing particles based on a review of the literature. The combined parameterization was applied under atmospheric conditions representative of the eastern United States using 3-dimensional fields of temperature, relative humidity, sulfate, nitrate, and ammonium, obtained from a recent Community Multiscale Air Quality model simulation. The resulting spatial distributions of γ were contrasted with three other parameterizations that have been applied in air quality models in the past and with atmospheric observational determinations of γ. Our results highlight a critical need for more laboratory measurements of γ at low temperature and high relative humidity to improve model simulations of N_2O_5 hydrolysis during wintertime conditions.

1 Introduction

Heterogeneous reactions of N_2O_5 have a substantial influence on gaseous and particulate pollutant concentrations (Dentener and Crutzen, 1993; Riemer et al., 2003; Aldener et al., 2006). To accurately simulate nighttime nitrogen chemistry and the resulting impacts on ozone, particulate nitrate, and nitrogen oxides, air quality models must contain a reliable parameterization of the heterogeneous reaction probability (γ), which is defined in a relative frequency sense as the fraction of collisions between

ACPD

7, 16119–16153, 2007

gaseous N_2O_5 molecules and particle surfaces that lead to the production of HNO_3.

Several recent laboratory studies demonstrate that γ varies substantially with temperature (T), relative humidity (RH), and particle composition (Mentel et al., 1999; Kane et al., 2001; Hallquist et al., 2003). Mechanistic explanations for these variations have been proposed (Mozurkewich and Calvert, 1988; Wahner et al., 1998; Hallquist et al., 2003), but the mechanisms are semi-quantitative at best and not yet suitable for inclusion in air quality models. In the absence of a quantitative heterogeneous reaction mechanism, some investigators have developed statistical parameterizations for γ based on laboratory data and incorporated those into air quality models. In a pioneering modeling study, Dentener and Crutzen (1993) selected 0.1 as a representative value of γ based on the available data at that time. Riemer et al. (2003) parameterized γ as a function of the particulate sulfate and nitrate content using laboratory data of Mentel et al. (1999). Most recently, Evans and Jacob (2005) modeled γ on sulfate particles as a function of RH and T using the laboratory data of Kane et al. (2001) and Hallquist et al. (2003), respectively.

In the present study, we build upon these past efforts to develop a parameterization of γ as a function of T, RH, particle composition, and phase state, for use in advanced air quality models. Our work has several advantages over previous studies: (1) our parameterization uses all published laboratory measurements of γ on ammoniated sulfate and nitrate particles; (2) rigorous statistical methods are employed (e.g., significance test of each independent variable, weighting of each data point by the measurement uncertainty, defining extrapolation limits) leading to a simple formula that captures the most important features in the laboratory data; and (3) phase changes are considered explicitly in our parameterization such that γ on aqueous particles exceeds that on solid particles.

2 Laboratory data

All the data used for our examination of γ with respect to T, RH, and particle composition come from laboratory work documented in the following publications: Mozurkewich and Calvert (1988); Hu and Abbatt (1997); Folkers (2001); Kane et al. (2001); Folkers et al. (2003); Hallquist et al. (2003); Badger et al. (2006a). For brevity, these documents will be referred to hereafter as MOZ88, HU97, FOL01, KAN01, FOL03, HAL03, and BAD06, respectively. To our knowledge, these seven publications contain all of the published laboratory measurements of γ on ammoniated sulfate and nitrate particles at conditions relevant to the troposphere. We focus on these particle compositions because they constitute a substantial portion of the aerosol surface area in continental air masses and because laboratory measurements of γ on these surfaces are relatively abundant. The impact of organic coatings on γ is an active area of research (Folkers et al., 2003; Anttila et al., 2006) and should be incorporated into future parameterizations.

Each publication contains a description of the procedures that were followed to determine γ from analytical measurements of the reactants and/or products of the heterogeneous reaction. In some cases, the laboratory procedures differ considerably from one another (e.g., FOL03 vs. HAL03); however, accounting for the possible impacts of procedural differences on the reported values of γ is beyond the scope of this work. Therefore, we used published values of γ directly rather than attempting to compute them from raw laboratory measurements.

2.1 Aqueous particles

Our review of the literature identified 67 published values of γ on aqueous particles, including 35 data points for NH_4HSO_4, 28 for $(NH_4)_2SO_4$, and 4 for NH_4NO_3 (see Table 1). Four MOZ88 data points on NH_4HSO_4 in the 40–60% RH range were removed from our analyses based on the discussion in HAL03, which notes that the points in question greatly exceed γ values from other studies. MOZ88 describes an artificial enhancement of γ at RH<40% due to small amounts of NH_3 evaporating from the

NH_4HSO_4 particle surfaces, and this artifact may also have influenced their data between 40–60% RH. Included in Table 1 is a HAL03 data point on $(NH_4)_2SO_4$ particles at 20% RH and 298 K. At those conditions, $(NH_4)_2SO_4$ is expected to be dry (Martin et al., 2003) but HAL03 reports a measurable increase in aerosol volume in these experiments relative to their own dry experiments at 20% RH. Therefore, this datum is retained for statistical modeling of the aqueous particle data.

Figure 1a to c summarize all 63 of the laboratory measurements used to develop our statistical model for aqueous particles, and illustrates the dependence of γ on RH, T, and particle composition. For all three compositions studied here, the most prominent feature, with a few exceptions, is that γ increases with RH. For a fixed RH and T, γ is highest on NH_4HSO_4, lowest on NH_4NO_3, and exhibits intermediate values on $(NH_4)_2SO_4$. A successful statistical model must capture these features of the laboratory data.

2.2 Dry particles

Our literature review also identified 24 published values of γ on dry particles, including 11 data points for NH_4HSO_4 and 13 for $(NH_4)_2SO_4$ (see Table 2). Measurements of γ on dry NH_4NO_3 were not found. All of the MOZ88 data points were removed from our analyses for reasons discussed above and in the footnotes of Table 2. Theoretically, none of the NH_4HSO_4 particles analyzed in KAN01 should be dry because their experiments began with wet particles and pure NH_4HSO_4 does not crystallize at 295 K (Martin et al., 2003). However, we include three KAN01 data points in Table 2 because of their extremely low γ values coupled with the knowledge that supersaturated aqueous NH_4HSO_4 particles are difficult to sustain below 22% RH (Tang and Munkelwitz, 1994). The $(NH_4)_2SO_4$ particles analyzed in KAN01 below 40% RH and in BAD06 below 34% RH were reported as dry, so they are included in Table 2. Similarly, six of the $(NH_4)_2SO_4$ data points from HAL03 are reported on dry particles. All of the data reported by HU97, FOL01, and FOL03 were obtained on aqueous particles, so those publications are not listed in Table 2.

An analysis of the 15 valid laboratory values of γ on dry particles indicates that they are generally lower than γ on aqueous particles. The very limited data reveal an apparent influence of RH and T on γ, which can be seen in Fig. 1d.

3 Methods

3.1 Statistical models for aqueous particles

The primary objective of this study is to derive a robust statistical parameterization for γ on aqueous particles using the data summarized in Fig. 1. Prior to our regression analyses, the laboratory data were transformed using the logit function:

$$\lambda = \ln\left(\gamma/(1-\gamma)\right)$$

This transformation ensures that all model estimates of γ lie between zero and one, which is consistent with the relative-frequency definition of γ. One regression equation was estimated from the union of NH_4HSO_4 and $(NH_4)_2SO_4$ data for which observations are most abundant. A model based on the NH_4NO_3 data was fit separately since those measurements were reported in a separate study from all the ammoniated sulfate data and include only four unique combinations of T and RH values (see FOL01 data in Table 1).

On NH_4HSO_4 and $(NH_4)_2SO_4$ particles, a dependence of γ on temperature is difficult to observe in the measurements. The only cross sections of data where temperature was varied over a large range are at 50% RH (see Fig. 1a and b). Along those cross sections, the γ values do not change monotonically with temperature. Based on the work by Hallquist et al. (2003), Evans and Jacob (2005), and our own data analyses, a temperature threshold, j, was applied within our statistical model. The threshold temperature variable is defined as:

$$T_j = \max(T - j, 0)$$

ACPD
7, 16119–16153, 2007

EGU

Our initial form of the statistical model for aqueous NH_4HSO_4 and $(NH_4)_2SO_4$ particles, denoted λ_1 and λ_2, respectively, is given by:

$$\lambda_1 = \beta_{10} + \beta_{11}RH + \beta_{12}T_j + \beta_{13}RH \times T_j + \beta_{14}RH^2 + \beta_{15}RH^3 + \varepsilon_1 \quad (1)$$

$$\lambda_2 = (\beta_{10} + \beta_{20}) + (\beta_{11} + \beta_{21})RH + (\beta_{12} + \beta_{22})T_j + (\beta_{13} + \beta_{23})RH \times T_j + (\beta_{14} + \beta_{24})RH^2 + (\beta_{15} + \beta_{25})RH^3 + \varepsilon_2 \quad (2)$$

The regression coefficients, β_{ik}, represent scalar quantities and the model errors, ε_i, were assumed to be normally and independently distributed. Higher order polynomial terms were considered for RH, but not T_j, based on our inspection of plots of λ versus RH and T. Note that during the regression analysis, Eqs. (1) and (2) were solved simultaneously using the combination of NH_4HSO_4 and $(NH_4)_2SO_4$ data. The extra coefficients – β_{20}, β_{21}, β_{22}, β_{23}, β_{24}, and β_{25} – in Eq. (2) were included to test whether the linear relationship between λ, RH, and T_j, differs significantly for different particle compositions.

Coefficients of the linear model were estimated using weighted least squares (Kutner et al., 2005). Each observation was assigned a weight, w, that is a function of the standard error values, σ, reported with each laboratory measurement of γ:

$$w = [\gamma(1-\gamma)]^2/\sigma^2 \quad (3)$$

These weights were derived based on a Taylor approximation for the estimate of the variance of λ (Casella and Berger, 2002, p. 241).

Stepwise model selection for regression analysis was used to determine which of the variables in Eqs. (1) and (2) are statistically significant. At each stage of the model selection process, the Akaike Information Criterion (AIC) was used to decide whether linear terms, cross product terms, and higher order terms should be included or excluded. This process was repeated for each integer value of j between 275 K and 295 K as well as for a model with no temperature threshold (i.e. j=0 K). The AIC value was used to determine the most parsimonious statistical model that best fits the data

with a minimum number of covariates (Akaike, 1973). This procedure yielded a model with four statistically significant terms and a threshold temperature of j=287 K. The individual equations for NH_4HSO_4 and $(NH_4)_2SO_4$ differ only in the intercept term.

$$\lambda_1 = \beta_{10} + \beta_{11}RH + \beta_{12}T_{287} + \varepsilon_1 \quad (4)$$

$$\lambda_2 = (\beta_{10} + \beta_{20}) + \beta_{11}RH + \beta_{12}T_{287} + \varepsilon_2 \quad (5)$$

The best-fit values and standard errors of each coefficient are given in Table 3. Several diagnostics were used to assess the adequacy of the regression function. Plots of the residuals from the linear model indicate the error terms are reasonably normally distributed. Correlation between the covariates is very low, indicating the effects of multicollinearity on the estimated regression parameters should not be a problem.

For aqueous NH_4NO_3 particles, all data were collected in a narrow temperature range so it was not possible to identify a temperature trend. The model for NH_4NO_3 was selected to match the form of Eq. (1), and is given by the following equation:

$$\lambda_3 = \beta_{30} + \beta_{31}RH + \varepsilon_3 \quad (6)$$

The estimated coefficients for this model are also given in Table 3. The estimated values of γ_1, γ_2, and γ_3, are back transformed to compute the reaction probability values for the three particle compositions.

$$\gamma_i = \frac{1}{1 + e^{-\lambda_i}} \quad i = 1,\ 2,\ 3 \quad (7)$$

The parameterized functions for γ are plotted on a log scale versus RH in the upper panel of Fig. 2 for a selected set of temperatures. The lower panel of Fig. 2 shows contour plots of the estimated γ values spanning the ranges of T and RH encountered in the lower troposphere. Each laboratory measurement is shown as a discrete point in the lower panel. Laboratory data are not available over the entire range of tropospheric conditions, so caution must be exercised when extrapolating parameterizations derived from the available data. For example, extrapolation of the regression equations to the

regime of low T and high RH yields γ values which exceed all of the lab measurements (e.g., γ_1>0.15). To prevent erroneous extrapolations when these functions are used in air quality models, such as the application in Sect. 4.3, the estimated γ values were constrained to be no greater than the maximum observed γ:

$$\begin{aligned} \gamma_1^* &= \min(\gamma_1, 0.08585) \\ \gamma_2^* &= \min(\gamma_2, 0.053) \\ \gamma_3^* &= \min(\gamma_3, 0.0154) \end{aligned} \tag{8}$$

These upper limits are depicted by horizontal gray lines in Fig. 2a–c, and the lightly-shaded irregular pentagons in the lower-right portions of Fig. 2d–f.

Extrapolation of Eqs. (4–7) must also be limited by thermodynamic considerations. At RH<32.8%, $(NH_4)_2SO_4$ crystallizes to form a solid phase (Martin et al., 2003) so γ_2 is expected to decline abruptly with decreasing RH across this phase boundary. The regions of Fig. 2b and e with RH lower than the crystallization relative humidity (CRH) are shaded to illustrate this limit. In contrast, aqueous droplets containing pure NH_4HSO_4 or pure NH_4NO_3 do not crystallize (Martin et al., 2003) so our equations for γ_1 and γ_3 may be applicable at very low RH.

Under the conditions of very high RH and low T encountered occasionally in the lower troposphere, particle-bound water will freeze to form ice (Martin, 2000). The point at which this phase change occurs is determined by the ratio of the saturation vapor pressure over ice (pw_{ice}) to that over water (pw_{water}). This portion of the phase diagram is shaded in the lower panel of Fig. 2, using the Goff-Gratch equations to compute pw_{ice} and pw_{water} (Goff and Gratch, 1946). As RH increases across this phase boundary, we expect γ to be far less than the upper limits imposed by Eq. (8).

3.2 Statistical model for dry particles

When the ambient RH is below the deliquescence relative humidity (DRH), ammoniated sulfate and nitrate can exist as dry particles that are devoid of liquid water. For dry particles, a separate parameterization is needed for γ. The statistical methodology

outlined in Sect. 3.1 was repeated using the 15 dry particle data points selected from Table 2 except, this time, higher order polynomial terms of RH were not considered due to the very limited sample size. The variable selection procedure yielded a model with three statistically significant terms and a threshold temperature of 293 K. Analogous to Eq. (2), extra coefficients were included to test whether the linear relationship between λ, RH, and T_j, differs for different particle compositions, but none of those coefficients were deemed significant. The model for dry particles (denoted with subscript "d" for dry) is given by

$$\lambda_d = \beta_{d0} + \beta_{d1} RH + \beta_{d2} T_{293} + \varepsilon_d \tag{9}$$

The best-fit values and standard errors of each coefficient are given in Table 3. The estimated values of λ_d can be back transformed using Eq. (7). As with the aqueous parameterizations, estimated γ values were constrained to be no greater than the maximum observed γ:

$$\gamma_d^* = \min(\gamma_d, 0.0124) \tag{10}$$

Recall that no laboratory measurements of γ on dry NH_4NO_3 were found, so Eqs. (9–10) are intended primarily for dry ammoniated sulfate particles.

3.3 Model for internally-mixed particles

In urban- and regional-scale air quality models, inorganic fine particles are often assumed to exist as an internal mixture of SO_4^{2-}, NO_3^-, NH_4^+, and H_2O (Wexler et al., 1994; Binkowski and Roselle, 2003). To date, laboratory measurements of γ on such mixtures have not been reported. As a provisional measure, it is useful to express γ as a molar-weighted average of the single-component parameterizations provided above. Assuming all of the NO_3^- is present as NH_4NO_3 and the leftover NH_4^+ is distributed

between $(NH_4)_2SO_4$ and NH_4HSO_4, we computed mole fractions

$$\begin{aligned} x_1 &= 1 - (x_2 + x_3) \\ x_2 &= \max\left(0, \min\left(1 - x_3, \tfrac{A}{N+S} - 1\right)\right) \\ x_3 &= \tfrac{N}{N+S} \end{aligned} \tag{11}$$

where x_i represents the molar concentration of component i normalized by the summed concentrations of NH_4HSO_4, $(NH_4)_2SO_4$, and NH_4NO_3; and A, N, and S, represent the molar concentrations of particle-phase NH_4^+, NO_3^-, and SO_4^{2-}, respectively. The limiting values of x_2 correspond to mixtures that are more acidic than NH_4HSO_4 or more alkaline than $(NH_4)_2SO_4$. Such compositions are rarely found in tropospheric fine particles, but were considered in Eq. (11) for completeness.

Using the above mole fractions as weighting factors, the reaction probability of N_2O_5 on mixed aqueous particles, $\gamma_{\mathrm{aq,mix}}$, can be computed as

$$\gamma_{\mathrm{aq,mix}} = \sum_{i=1}^{3} x_i \gamma_i^* \tag{12}$$

where γ_i^* is defined in Eq. (8). The corresponding expression for mixed dry particles is

$$\gamma_{d,\mathrm{mix}} = (x_1 + x_2)\gamma_d^* + x_3 \cdot \min(\gamma_d^*, \gamma_3^*) \tag{13}$$

In the absence of laboratory measurements on dry NH_4NO_3 particles, the min function is used in Eq. (13) to reflect our expectation that γ on dry NH_4NO_3 particles is similar to γ on dry ammoniated sulfate particles, but should not exceed γ on aqueous NH_4NO_3 particles.

No laboratory measurements of γ on particles containing a mixture of ice and ammoniated sulfate or nitrate were found, but γ on pure ice has been studied extensively for stratospheric applications (e.g., Leu, 1988; Hanson and Ravishankara, 1991). A representative γ value of 0.02 was selected from those data (IUPAC, 2006). This fixed value was applied to all ice-containing particles in the present study.

$$\gamma_{\mathrm{ice,mix}} = 0.02 \tag{14}$$

4 Results

4.1 Mechanistic evaluation

Our statistical parameterizations capture all prominent features of the laboratory data and are qualitatively consistent with the ionic hydrolysis mechanism proposed by Mozurkewich and Calvert (1988) and extended by Wahner et al. (1998):

Condensation $N_2O_{5(g)} \rightarrow N_2O_{5(aq)}$ (R1a)

Evaporation $N_2O_{5(aq)} \rightarrow N_2O_{5(g)}$ (R1b)

Dissolution $N_2O_{5(aq)} \rightarrow NO_2^+ + NO_3^-$ (R2a)

Recombination $NO_2^+ + NO_3^- \rightarrow N_2O_{5(aq)}$ (R2b)

Ion hydrolysis $NO_2^+ + H_2O \rightarrow 2H^+ + NO_3^-$ (R3)

First, the aqueous parameterizations of γ increase with RH at each temperature for all three particle compositions (see Fig. 2a–c). This is consistent with the KAN01 and FOL01 data (see Fig. 1a–c), which indicate that aerosol water content controls γ via the dissolution step R2a. Second, the parameterization of γ on NH_4HSO_4 exceeds that on $(NH_4)_2SO_4$ (i.e., $\gamma_1 > \gamma_2$) by 42 to 62% due to the constraints imposed in Eq. (8) and the negative value of our β_{20} coefficient. This result is consistent with the KAN01 and HAL03 data (compare Fig. 1a and b). Kane et al. (2001) speculate that the rise in γ may be due to the small amount of H^+ in NH_4HSO_4 solutions, which could catalyze reaction R2a (Robinson et al., 1997). Third, the parameterizations of γ_1 and γ_2 decrease with increasing temperature for $T > 289$ K. This is consistent with the MOZ88 and HAL03 data (see vertical transects at 50%, 66%, and 76% RH in Fig. 1a, and at 50% RH in Fig. 1b). Mozurkewich and Calvert (1988) speculate that this negative temperature dependence may be due to the N_2O_5 evaporation rate (R1b) increasing faster with temperature than the N_2O_5 dissolution rate (R2a).

Fourth, the parameterization of γ on NH_4NO_3 is lower than that on $(NH_4)_2SO_4$ (i.e., $\gamma_3<\gamma_2$). This can be seen most clearly by comparing Fig. 2c with the 293 and 298 K isotherms in Fig. 2b because all of the NH_4NO_3 measurements were collected in that temperature range. This "nitrate effect" is described in detail by Mentel et al. (1999), and is attributed to an enhanced rate of N_2O_5 recombination (R2b) in aqueous particles composed of NO_3^-. Note that the NO_3^- concentration leading to recombination is dominated by the substrate composition rather than the small amount which comes from N_2O_5 dissolution. Comparing our parameterizations of γ_2 and γ_3 over the ranges of T and RH where NH_4NO_3 lab data are available (i.e., $293<T<298$ K and $50<RH<80\%$), we see that the nitrate effect ranges from a factor of 1.4 to 4.4. This rather broad range is due to the larger RH dependence in Eq. (6) versus (5) (compare β_{31} with β_{11} in Table 3). More importantly, the nitrate effect deduced from our analyses is much less pronounced than the factor of ten applied in model simulations by Riemer et al. (2003). Our result is probably more appropriate for continental air masses, because it is derived from a comparison between $(NH_4)_2SO_4$ and NH_4NO_3 particles rather than a comparison between Na_2SO_4 and $NaNO_3$ particles.

Fifth, our parameterization of γ on aqueous ammoniated sulfate is 1.2–9.0 times greater than that on dry particles within the RH range where those components can exist in either a solid or aqueous phase due to hysteresis (i.e., $\gamma_1>\gamma_d$ and $\gamma_2>\gamma_d$ for CRH $<RH<$DRH). This result is consistent with the HAL03 data, in which γ on wet $(NH_4)_2SO_4$ was found to be 1.2–13 times greater than that on dry $(NH_4)_2SO_4$ (compare 5 paired values in Tables 1 and 2). The difference in γ on dry versus wet particles can be attributed to the absence of water in the dry particles, which prohibits dissolution. Presumably, the reaction on dry particles proceeds in a very different manner than the ionic hydrolysis mechanism outlined above. One curious aspect of the γ_d parameterization is its dependence on RH (see Eq. 9). One would expect the heterogeneous uptake of N_2O_5 on dry particles to be independent of RH because RH does not affect the water content of solid particles. The observed and parameterized dependence of γ_d on RH may indicate that homogeneous gas-phase reactions between

N_2O_5 and water vapor were taking place during the laboratory experiments. A more detailed exploration of this possibility is warranted, but is beyond the scope of our study.

4.2 Statistical evaluation

Figure 3 illustrates a comparison between the parameterized γ values and the underlying laboratory data used for statistical modeling. Out of the 31 aqueous NH_4HSO_4 data points, 16 are fit within a factor of 1.25 and 23 within a factor of two (see Fig. 3a). The remaining eight points are overestimated by Eq. (4). Four of these are KAN01 data points with RH between 29 and 37%, which is in the metastable regime where the NH_4HSO_4 phase is very sensitive to trace impurities. Figure 6 in KAN01 shows the same four points falling below their best-fit line, while one data point in this RH range has a much higher γ value. It is possible that crystallization occurred during a subset of their experiments leading to the four low γ measurements. Figure 3a also reveals that Eq. (4) overestimates two HAL03 data points by a factor of three. Those values were measured at 268 and 273 K, but are a factor of three lower than the HAL03 observations at the surrounding temperatures of 263 and 288 K. To fit all four of these γ values would require a third order polynomial of temperature, but such a term would have no physical basis. Instead, Eq. (4) yields a fixed value of 0.042 for all 4 data points because they are all below the threshold temperature of 289 K. Finally, Fig. 3a shows one FOL03 data point that is overestimated by more than a factor of two. This γ value was measured at 79.7% RH, but is nearly identical to the γ measurement at 60.1% RH reported by the same authors (see Table 1). The lack of RH dependence exhibited by these FOL03 points is counter to the other studies (see Fig. 1a) and is therefore not captured in our parameterization.

Out of the 28 aqueous $(NH_4)_2SO_4$ data points, 13 are fit within a factor of 1.25 and 22 within a factor of two (see Fig. 3b). All four data points that Eq. (5) overestimates by more than a factor of two are from KAN01 and in the metastable RH regime (42, 45, 48, and 62% RH). Figure 5 in KAN01 shows the same four points falling below their best-fit line, while three data points in this RH range have much higher γ values. As noted

by Hallquist et al. (2003) and analogous to our line of reasoning above, we speculate that crystallization occurred during a subset of the KAN01 $(NH_4)_2SO_4$ experiments leading to the four low γ measurements. Figure 3b also reveals two HU97 data points that we underestimate by a factor of three or more. A number of authors (e.g., Kane et al., 2001; Hallquist et al., 2003) have commented that the HU97 data are unlike those reported in any other study, both in their magnitude and RH dependence, but no physical explanation could be found to justify the exclusion of these data from our statistical model. Given the large differences compared to other laboratory data, we do not expect our parameterization to fit the HU97 data well and this expectation is verified in Fig. 3b.

Figure 3c shows excellent agreement between the fitted and observed γ values on aqueous NH_4NO_3 particles, with Eq. (6) capturing all four data points within ±7%. Figure 3d reveals good agreement between Eq. (9) and the dry particle data. Out of the 15 data points, 8 are fit within a factor of 1.25 and 13 within a factor of two. One of the outlying data points has an extremely large measurement uncertainty (see HAL03 datum at 308 K in Table 2) so our weighted regression model is not expected to capture this point. Equation (9) reproduces the other outlying point – from KAN01 at 8% RH – within two times the measurement uncertainty.

In Fig. 3e, we summarize a comparison between all of the fitted and observed γ values used to develop our regression equations. Among the 78 data points reported in seven different laboratory studies, our parameterizations reproduce 53% within a factor of 1.25 and 79% within a factor of two. For comparison, we contrasted this performance with the T- and RH-dependent parameterization reported by Evans and Jacob (2005) for γ on $(NH_4)_2SO_4$ particles (referred to hereafter as EJ05). In the process, we discovered a typographical error in Table 1 of that paper. The form of their equation should read $\gamma = \alpha \times 10^{-\beta}$ but the negative sign was omitted in the publication (Mathew Evans, personal communication). Figure 3f summarizes the EJ05 performance after correction of the typographical error. When compared against all 40 $(NH_4)_2SO_4$ data points (dry and wet), EJ05 underestimates half of them by 15% or more whereas our parameteri-

zation exhibits a smaller median relative bias (+5%). The EJ05 parameterization is not intended for NH_4HSO_4 particles and an erroneous application of EJ05 to such acidic particle surfaces would underestimate most of the NH_4HSO_4 data points by nearly a factor of 2 (see triangular symbols in Fig. 3f). Similarly, EJ05 should not be applied to NH_4NO_3 particles because it was not designed to capture the nitrate effect on γ (see plus symbols in Fig. 3f).

4.3 Atmospheric implications

To illustrate the atmospheric relevance of this work, we applied the parameterizations developed here to conditions representative of the eastern United States using 3-dimensional fields of T, RH, SO_4^{2-}, NO_3^-, and NH_4^+, obtained from a recent numerical simulation using the Community Multiscale Air Quality (CMAQ) modeling system with 12 km horizontal grid spacing (Appel et al., 2007[1]). In that model application, transitions in the aerosol phase state were not simulated. To utilize all of the parameterizations developed in this study, we assume here that the modeled particles are wet above their CRH and dry below their CRH. This is a reasonable assumption because several field campaigns have demonstrated that tropospheric particles often retain water well below their DRH (Rood et al., 1989; Santarpia et al., 2004; Khlystov et al., 2005). The CRH for an internally mixed particle composed of SO_4^{2-}, NO_3^-, and NH_4^+ was calculated using the equation for complete crystallization by Martin et al. (2003). Although that equation was only validated at 293 K, we applied it at all T because there currently exists very little data to justify a temperature-dependent CRH (see discussion by Schlenker et al., 2004). To compute γ over the full range of conditions encountered in the atmosphere,

[1] Appel, K. W., Bhave, P. V., Gilliland, A. B., Sarwar, G., and Roselle, S. J.: Evaluation of the Community Multiscale Air Quality (CMAQ) model version 4.5: Uncertainties and sensitivities impacting model performance. Part II: Particulate matter, Atmos. Environ., in review, 2007.

γ_{ambient}, we applied Eqs. (12–14) as follows:

$$\gamma_{\text{ambient}} = \begin{cases} \gamma_{d,\text{mix}} & \text{RH<CRH} \\ \gamma_{\text{ice,mix}} & \text{RH>IRH} \\ \gamma_{\text{aq,mix}} & \text{otherwise} \end{cases} \tag{15}$$

where IRH is the relative humidity of ice formation, which varies with temperature (see discussion in Section 3.1).

Values of γ_{ambient} were computed for each hour of January, February, July, and August 2001, using T, RH, SO_4^{2-}, NO_3^-, and NH_4^+ in each CMAQ grid cell. For comparison, we also computed hourly spatial fields of γ on NH_4HSO_4 (i.e., γ_1^*), $(NH_4)_2SO_4$ (i.e., γ_2^* when RH ≥32.8% and γ_d^* otherwise), and NH_4NO_3 (i.e., γ_3^*), each with the IRH constraint imposed, as well as three other parameterizations of γ that have been applied in air quality models in the past. For illustrative purposes, the hourly γ values were averaged over two-month periods representative of the winter (January–February 2001) and summer (July–August 2001). When averaging hourly values, we included only the nighttime hours of 04:00–09:00 GMT because N_2O_5 concentrations are negligible in the daylight (Brown et al., 2003a) so values of γ at those times have no practical importance. Though vertical distributions of γ were computed, we focused our attention on the model layer that is 75–150 m above the surface because the CMAQ results indicate that the product of N_2O_5 and aerosol surface area is highest in this layer during both the summer and winter periods. Recall that the N_2O_5 hydrolysis rate is proportional to this product (Riemer et al., 2003). Vertical profiles of NO_3 and N_2O_5 measured by Stutz et al. (2004) and Brown et al. (2007), respectively, support our decision to focus on γ at ~100 m above the surface.

Figure 4 displays results of the above calculations for the January–February 2001 period. Across the eastern U.S., values of γ_{ambient} range from 0.02 over the Midwest to 0.05 over Florida (see Fig. 4d). Low values over the Midwest result from high NO_3^- concentrations, typical of this region during winter, combined with below-freezing temperatures and high RH that occasionally exceeds the IRH. The high γ_{ambient} values

over Florida result from low NO_3^- concentrations coupled with relatively warm temperatures. Comparing Fig. 4d with e, it can be seen that our $\gamma_{ambient}$ values fall below the fixed value of 0.1 used in the early work by Dentener and Crutzen (1993) which is now recognized as an upper estimate of γ (Evans and Jacob, 2005). Comparing Fig. 4d with f, we see that the γ parameterization by Riemer et al. (2003) is consistently lower than $\gamma_{ambient}$. The Riemer parameterization has an upper bound of 0.02, based on measurements of γ on Na_2SO_4 and $NaHSO_4$ particles (Mentel et al., 1999). As noted above, our parameterization is more appropriate for continental air masses because it is derived from measurements on ammoniated particles rather than sodium-containing particles. Moreover, the Riemer parameterization does not depend on T and RH due to insufficient data at the time of that study.

The comparison between $\gamma_{ambient}$ and EJ05 is the most intriguing (compare Fig. 4d and g) because EJ05 is the current parameterization of choice in many regional- and global-chemistry models such as CMAQv4.6 and GEOS-CHEM. Across the northern half of the domain, EJ05 often exceeds 0.10 whereas $\gamma_{ambient}$ is between 0.02 and 0.06. At lower latitudes, EJ05 exceeds $\gamma_{ambient}$ by 0.01 to 0.02. Recognizing that $\gamma_{ambient}$ is suppressed by the nitrate effect whereas EJ05 is not, a more equitable comparison is between EJ05 and our parameterization of γ on $(NH_4)_2SO_4$ (i.e., Fig. 4g versus b). Surprisingly, this comparison also revealed rather large differences. The main reason for differences in the northern latitudes is that our parameterization was bounded by the maximum laboratory value of 0.053 (see Fig. 2b and e) whereas EJ05 yields very large values when extrapolated to low T and high RH conditions. In addition, our values of γ in the north and along the Appalachian Mountains are suppressed by ice formation (see upper-left corner of Fig. 4b for example) whereas the effects of that phase transition are not considered in the EJ05 parameterization. In fact, the very highest values of γ (~0.13) are obtained when EJ05 is extrapolated to the regime where ice formation is favored. In the southern half of the domain, EJ05 exceeds γ_2^* by 0.02 to 0.03. These locations are characterized by average nighttime conditions of 80% RH and 280 K, where EJ05 yields a value of 0.08 and our parameterization reaches its upper-limit

value of 0.053.

In the summer, $\gamma_{ambient}$ ranges from 0.01 over Texas and Oklahoma to 0.07 over the Appalachian Mountains. The lowest values correspond to the portion of our domain where the nighttime average temperature was highest (302 K), RH was lowest (60%), and the particle compositions were dominated by $(NH_4)_2SO_4$ (x_2=0.9). Over the Appalachian Mountains, high values of $\gamma_{ambient}$ resulted from the particle compositions being dominated by NH_4HSO_4 (x_1=0.8) along with T<290 K and RH>80%. Across the entire domain, $\gamma_{ambient}$ and EJ05 were in very good agreement except in locations where x_1=0.8. Under those acidic conditions, $\gamma_{ambient}$ exceeded EJ05 by nearly 0.02 as would be expected from a comparison of Fig. 3e and f.

5 Discussion

5.1 Comparisons with atmospheric data

Historically, attempts to estimate γ from atmospheric observations were obstructed by the inability to measure ambient N_2O_5 concentrations. This obstacle was overcome by Brown et al. (2001), leading to ambient measurements of N_2O_5 in a handful of intensive field campaigns (Brown et al., 2003a; Brown et al., 2004; Wood et al., 2005; Brown et al., 2006; Matsumoto et al., 2006; Ayers and Simpson, 2006). Brown et al. (2003b) also developed an innovative method for estimating γ from simultaneous, high-resolution measurements of N_2O_5, NO_3, NO_2, O_3, and aerosol surface area. Applications of this technique have been reported in two field campaigns to date, yielding ambient estimates of γ=0.03±0.02 in the marine boundary layer off the coast of New England during summer 2002 (Aldener et al., 2006) and γ=0.017±0.004 over Ohio and western Pennsylvania during summer 2004 (Brown et al., 2006). Using the CMAQ results which simulated July – August 2001, our parameterization yields slightly larger values: $\gamma_{ambient}$=0.05 off the New England coast, and 0.03–0.05 over Ohio and western Pennsylvania. However, as mentioned in Section 2, our parameterization neglects the

influence of organic coatings on $\gamma_{ambient}$. Some limited laboratory and field evidence suggests that the organic influence is very important (Folkers et al., 2003; Anttila et al., 2006; Brown et al., 2006) and additional research in that area should help close the gap between the observation-based and statistically-parameterized estimates of γ during the summer.

Several modeling studies concur that gaseous and particulate pollutant concentrations are far more sensitive to γ during the winter than during summer (Dentener and Crutzen, 1993; Evans and Jacob, 2005; Gilliland et al., 2006). However, N_2O_5 has seldom been measured in wintertime field campaigns (Wood et al., 2005; Ayers and Simpson, 2006) and neither of those campaigns collected the full suite of measurements required to estimate γ. Moreover, it is not clear that the observation-based estimation method mentioned above will be successful during winter months because the underlying steady state approximation is not applicable at cold temperatures (Brown et al., 2003b). Thus, our ability to evaluate the statistical parameterizations of γ against atmospheric data is hindered during winter months which, unfortunately, correspond to when the heterogeneous reaction probability has maximum importance.

5.2 Critical gaps in the laboratory data

Our statistical analysis of the laboratory data and our assessment of the atmospheric implications have helped to identify the most important areas where more laboratory measurements of γ are needed. First, laboratory studies at low T and high RH conditions are of utmost importance. This need is motivated by the substantial differences between Fig. 4b and g, which arise from different extrapolations of the available laboratory data to typical winter conditions. A set of laboratory measurements at ~260 K with RH increasing from 50–95% would be particularly illuminating as it would help fill in the data gap mentioned above and test our hypothesis that γ decreases abruptly at the phase boundary between liquid water and ice. A transect of laboratory measurements at ~85% RH with T decreasing from 295 to 260 K would also be valuable to double-check the validity of the temperature threshold in Eqs. (4–5). It is important

to emphasize that no laboratory measurements of γ on aqueous $(NH_4)_2SO_4$ particles are available below 288 K (see Fig. 2e). Such data are essential for atmospheric modeling during winter periods, especially given the fact that there are no ambient data to evaluate our statistical parameterizations during winter months.

Second, there is a need for more laboratory data on aqueous NH_4NO_3 particles. The available measurements adequately characterize the regime of 293–298 K and 50–80% RH (see Fig. 2f). In the atmosphere, NH_4NO_3 concentrations are highest in the winter because of low SO_4^{2-} concentrations and because NH_4NO_3 formation is most favorable at low T and high RH (Stelson and Seinfeld, 1982). Therefore, future experiments on NH_4NO_3 particles should be conducted at conditions representative of winter. Third, a few laboratory experiments ought to be conducted on internally-mixed particles consisting of aqueous SO_4^{2-}, NO_3^-, and NH_4^+. Such experiments would help evaluate and refine the simple mixing rule given in Eq. (12). Fourth, a few measurements are needed on particles containing a mixture of ice and ammoniated sulfate or nitrate. As noted in Sect. 3.3, in the absence of such measurements, we opted to use a γ value for pure ice in the present study (see Eq. 14).

Although there are far fewer measurements of γ on dry particle surfaces than on wetted surfaces, we believe that additional experiments on dry particles will not be very valuable. In our analyses of the 3-dimensional CMAQ fields, the ambient RH fell below the internally-mixed CRH in only 0.02 and 0.7% of the grid cells during summer and winter, respectively. However, this conclusion may require reevaluation if future studies elucidate a strong temperature dependence in the CRH of internally mixed particles.

6 Conclusions

We have developed a comprehensive parameterization for the heterogeneous reaction probability of N_2O_5 as a function of RH, T, particle composition, and phase state, for use in advanced air quality models. We used all published measurements of γ on ammoniated sulfate and nitrate particles, which were compiled from seven different

laboratory studies. The final equations are relatively simple, non-linear functions of RH and T that were selected in an objective and statistically rigorous manner. Our parameterization reproduced 79% of the laboratory data within a factor of two and 53% within a factor of 1.25. To our knowledge, this is the first parameterization in which phase changes are considered explicitly such that γ on aqueous particles exceeds that on solid particles. It is also the first parameterization to capture the ~50% enhancement of γ on NH_4HSO_4 particle surfaces relative to $(NH_4)_2SO_4$. Another important result comes from our reevaluation of the nitrate effect using laboratory data on ammoniated particles. That effect, which was previously considered to decrease γ by a factor of ten (Mentel et al., 1999; Riemer et al., 2003), is now believed to be a factor of 1.4 to 4.4.

Our parameterization was applied under winter and summer conditions representative of the eastern United States using 3-dimensional fields of T, RH, SO_4^{2-}, NO_3^-, and NH_4^+ obtained from a recent CMAQ model simulation. The resulting spatial distributions of γ were contrasted with three other parameterizations that have been applied in air quality models in the past. Our ambient estimates of γ fall between the upper value proposed by Dentener and Crutzen (1993) and the rather low values used by Riemer et al. (2003). Under winter conditions, large differences were found between our parameterization and that of Evans and Jacob (2005). Our parameterization yields summertime values that are slightly larger than the ambient-observational estimates of Aldener et al. (2006) and Brown et al. (2006). These comparisons helped us identify critical gaps in the laboratory data that will be most valuable for future refinements of the γ parameterization.

Acknowledgements. We would like to thank our colleagues for their help and advice. These include H. Zhang and H. Wang, Professors of Statistics at North Carolina State University; S. Clegg, University of East Anglia; J. Swall, Atmospheric Sciences Modeling Division, Air Resources Laboratory, National Oceanic and Atmospheric Administration; and N. Riemer, State University of New York, Stonybrook. We also thank M. Evans of University of Leeds, M. Hallquist of Göteborg University, and R. A. Cox of University of Cambridge, for initial discussions concerning this research.

The research presented here was performed under the Memorandum of Understanding between the U.S. Environmental Protection Agency (EPA) and the U.S. Department of Commerce's National Oceanic and Atmospheric Administration (NOAA) and under agreement number DW13921548. This work constitutes a contribution to the NOAA Air Quality Program. Although it has been reviewed by EPA and NOAA and approved for publication, it does not necessarily reflect their policies or views.

References

Akaike, H.: Information theory and an extension of the maximum likelihood principle. In Proc. 2nd Int. Symp. Information Theory, eds B. N. Petrov and F. Csáki, Budapest, 267–281, 1973.

Aldener, M., Brown, S. S., Stark, H., Williams, E. J., Lerner, B. M., Kuster, W. C., Goldan, P. D., Quinn, P. K., Bates, T. S., Fehsenfeld, F. C., and Ravishankara, A. R.: Reactivity and loss mechanisms of NO_3 and N_2O_5 in a polluted marine environment: Results from in situ measurements during New England Air Quality Study 2002, J. Geophys. Res., 111, D23S73, doi:10.1029/2006JD007252, 2006.

Anttila, T., Kiendler-Scharr, A., Tillmann, R., and Mentel, T. F.: On the reactive uptake of gaseous compounds by organic-coated aqueous aerosols: Theoretical analysis and application to the heterogeneous hydrolysis of N_2O_5, J. Phys. Chem. A, 110, 10 435–10 443, 2006.

Ayers, J. D. and Simpson, W. R.: Measurements of N_2O_5 near Fairbanks, Alaska, J. Geophys. Res., 111, D14309, doi:10.1029/2006JD007070, 2006.

Badger, C. L., Griffiths, P. T., George, I., Abbatt, J. P. D., and Cox, R. A.: Reactive uptake of N_2O_5 by aerosol particles containing mixtures of humic acid and ammonium sulfate, J. Phys. Chem. A, 110, 6986–6994, 2006a.

Badger, C. L., George, I., Griffiths, P. T., Braban, C. F., Cox, R. A., and Abbatt, J. P. D.: Phase transitions and hygroscopic growth of aerosol particles containing humic acid and mixtures of humic acid and ammonium sulphate, Atmos. Chem. Phys., 6, 755–768, 2006b.

Binkowski, F. S. and Roselle, S. J.: Models-3 Community Multiscale Air Quality (CMAQ) model aerosol component – 1. Model description, J. Geophys. Res., 108, 4183, doi:10.1029/2001JD001409, 2003.

Brown, S. S., Stark, H., Ciciora, S. J., and Ravishankara, A. R.: In-situ measurement of atmo-

spheric NO_3 and N_2O_5 via cavity ring-down spectroscopy, Geophys. Res. Lett., 28, 3227–3230, 2001.

Brown, S. S., Stark, H., Ryerson, T. B., Williams, E. J., Nicks, D. K., Trainer, M., Fehsenfeld, F. C., and Ravishankara, A. R.: Nitrogen oxides in the nocturnal boundary layer: Simultaneous in situ measurements of NO_3, N_2O_5, NO_2, NO, and O_3, J. Geophys. Res., 108, 4299, doi:10.1029/2002JD002917, 2003a.

Brown, S. S., Stark, H., and Ravishankara, A. R.: Applicability of the steady state approximation to the interpretation of atmospheric observations of NO_3 and N_2O_5, J. Geophys. Res., 108, 4539, doi:10.1029/2003JD003407, 2003b.

Brown, S. S., Dibb, J. E., Stark, H., Aldener, M., Vozella, M., Whitlow, S., Williams, E. J., Lerner, B. M., Jakoubek, R., Middlebrook, A. M., DeGouw, J. A., Warneke, C., Goldan, P. D., Kuster, W. C., Angevine, W. M., Sueper, D. T., Quinn, P. K., Bates, T. S., Meagher, J. F., Fehsenfeld, F. C., and Ravishankara, A. R.: Nighttime removal of NO_x in the summer marine boundary layer, Geophys. Res. Lett., 31, L07108, doi:10.1029/2004GL019412, 2004.

Brown, S. S., Ryerson, T. B., Wollny, A. G., Brock, C. A., Peltier, R., Sullivan, A. P., Weber, R. J., Dube, W. P., Trainer, M., Meagher, J. F., Fehsenfeld, F. C., and Ravishankara, A. R.: Variability in nocturnal nitrogen oxide processing and its role in regional air quality, Science, 311, 67–70, 2006.

Brown, S. S., Dubé, W. P., Osthoff, H. D., Wolfe, D. E., Angevine, W. M., and Ravishankara, A. R.: High resolution vertical distributions of NO_3 and N_2O_5 through the nocturnal boundary layer, Atmos. Chem. Phys., 7, 139–149, 2007, http://www.atmos-chem-phys.net/7/139/2007/.

Casella, G. and Berger, R. L.: Statistical Inference, 2nd edition, Duxbury, Pacific Grove, CA, 2002.

Dentener, F. J. and Crutzen, P. J.: Reaction of N_2O_5 on tropospheric aerosols: Impact on the global distributions of NO_x, O_3, and OH, J. Geophys. Res., 98, 7149–7163, 1993.

Evans, M. J. and Jacob, D. J.: Impact of new laboratory studies of N_2O_5 hydrolysis on global model budgets of tropospheric nitrogen oxides, ozone and OH, Geophys. Res. Lett., 32, L09813, doi:10.1029/2005GL022469, 2005.

Folkers, M.: Bestimmung der reaktionswahrscheinlichkeit von N_2O_5 an troposhärisch relevanten aerosolen, Ph.D. Thesis, Universität Köln, 2001.

Folkers, M., Mentel, Th. F., and Wahner, A.: Influence of an organic coating on the reactivity of aqueous aerosols probed by the heterogeneous hydrolysis of N_2O_5, Geophys. Res. Lett.,

30, 1644, doi:10.1029/2003GL017168, 2003.
Fried, A., Henry, B. E., Calvert, J. G., and Mozurkewich, M.: The reaction probability of N_2O_5 with sulfuric acid aerosols at stratospheric temperatures, J. Geophys. Res., 99, 3517–3532, 1994.
Gilliland, A. B., Appel, K. W., Pinder, R. W., and Dennis, R. L.: Seasonal NH_3 emissions for the continental United States: Inverse model estimation and evaluation, Atmos. Environ., 40, 4986–4998, 2006.
Goff, J. A. and Gratch, S.: Low-pressure properties of water from −160 to 212F, in Transactions of the American society of heating and ventilating engineers, presented at the 52nd annual meeting of the American society of heating and ventilating engineers, New York, 95–122, 1946.
Hallquist, M., Stewart, D. J., Stephenson, S. K., and Cox, R. A.: Hydrolysis of N_2O_5 on sub-micron sulfate aerosols, Phys. Chem. Chem. Phys., 5, 3453–3463, 2003.
Hanson, D. R. and Ravishankara, A. R.: The reaction probabilities of $ClONO_2$ and N_2O_5 on polar stratospheric cloud materials, J. Geophys. Res., 96, 5081–5090, 1991.
Hu, J. H. and Abbatt, J. P. D.: Reaction probabilities for N_2O_5 hydrolysis on sulfuric acid and ammonium sulfate aerosols at room temperature, J. Phys. Chem. A, 101, 871–878, 1997.
IUPAC Subcommittee on gas kinetic data evaluation: Data sheet H23, http://www.iupac-kinetic.ch.cam.ac.uk/, revised 15 August, 2006.
Kane, S. M., Caloz, F., and Leu, M.-T.: Heterogeneous uptake of gaseous N_2O_5 by $(NH_4)_2SO_4$, NH_4HSO_4, and H_2SO_4 aerosols, J. Phys. Chem. A, 105, 6465–6470, 2001.
Khlystov, A., Stanier, C. O., Takahama, S., and Pandis, S. N.: Water content of ambient aerosol during the Pittsburgh Air Quality Study, J. Geophys. Res., 110, D07S10, doi:10.1029/2004JD004651, 2005.
Kutner, M. H., Nachtshein, C. J., Neter, J., and Li, W.: Applied Linear Statistical Models, 5th edition, McGraw-Hill, New York, 2005.
Leu, M.-T.: Heterogeneous reactions of N_2O_5 and HCl on ice surfaces: implications for Antarctic ozone depletion, Geophys. Res. Lett., 15, 851–854, 1988.
Martin, S. T.: Phase transitions of aqueous atmospheric particles, Chem. Rev., 100, 3403–3453, 2000.
Martin, S. T., Schlenker, J. C., Malinowski, A., Hung, H.-M., and Rudich, Y.: Crystallization of atmospheric sulfate-nitrate-ammonium particles, Geophys. Res. Lett., 30, 2102, doi:10.1029/2003GL017930, 2003.

Matsumoto, J., Imagawa, K., Imai, H., Kosugi, N., Ideguchi, M., Kato, S., and Kajii, Y.: Nocturnal sink of NO_x via NO_3 and N_2O_5 in the outflow from a source area in Japan, Atmos. Environ., 40, 6294–6302, 2006.
Mentel, T. F., Sohn, M., and Wahner, A.: Nitrate effect in the heterogeneous hydrolysis of dinitrogen pentoxide on aqueous aerosols, Phys. Chem. Chem. Phys., 1, 5451–5457, 1999.
Mozurkewich, M. and Calvert, J. G.: Reaction probability of N_2O_5 on aqueous aerosols, J. Geophys. Res., 93, 15 889–15 896, 1988.
Riemer, N., Vogel, H., Vogel, B., Schell, B., Ackermann, I., Kessler, C., and Hass, H.: Impact of the heterogeneous hydrolysis of N_2O_5 on chemistry and nitrate aerosol formation in the lower troposphere under photosmog conditions, J. Geophys. Res., 108, 4144, doi:10.1029/2002JD002436, 2003.
Robinson, G. N., Worsnop, D. R., Jayne, J. T., Kolb, C. E., Davidovits, P.: Heterogeneous uptake of $ClONO_2$ and N_2O_5 by sulfuric acid solutions, J. Geophys. Res., 102, 3583–3601, 1997.
Rood, M. J., Shaw, M. A., Larson, T. V., and Covert, D. S.: Ubiquitous nature of ambient metastable aerosol, Nature, 337, 537–539, 1989.
Santarpia, J. L., Li, R., and Collins, D. R.: Direct measurement of the hydration state of ambient aerosol populations, J. Geophys. Res., 109, D18209, doi:10.1029/2004JD004653, 2004.
Schlenker, J. C., Malinowski, A., Martin, S. T., Hung, H.-M., and Rudich, Y.: Crystals formed at 293 K by aqueous sulfate-nitrate-ammonium-proton aerosol particles, J. Phys. Chem. A, 108, 9375–9383, 2004.
Stelson, A. W. and Seinfeld, J. H.: Relative humidity and temperature dependence of the ammonium nitrate dissociation constant, Atmos. Environ., 16, 983–992, 1982.
Stutz, J., Alicke, B., Ackermann, R., Geyer, A., White, A., and Williams, E.: Vertical profiles of NO_3, N_2O_5, O_3, and NO_x in the nocturnal boundary layer: 1. Observations during the Texas Air Quality Study 2000, J. Geophys. Res., 109, D12306, doi:10.1029/2003JD004209, 2004.
Tang, I. N. and Munkelwitz, H. R.: Water activities, densities, and refractive indices of aqueous sulfates and sodium nitrate droplets of atmospheric importance, J. Geophys. Res., 99, 18 801–18 808, 1994.
Wahner, A., Mentel, T. F., Sohn, M., and Stier, J.: Heterogeneous reaction of N_2O_5 on sodium nitrate aerosol, J. Geophys. Res., 103, 31 103–31 112, 1998.
Wexler, A. S., Lurmann, F. W., and Seinfeld, J. H.: Modelling urban and regional aerosols – I. Model development. Atmos. Environ., 28, 531–546, 1994.
Wood, E. C., Bertram, T. H., Wooldridge, P. J., and Cohen, R. C.: Measurements of N_2O_5, NO_2,

and O_3 east of the San Francisco Bay, Atmos. Chem. Phys., 5, 483–491, 2005, http://www.atmos-chem-phys.net/5/483/2005/.

Table 1. Laboratory measurements of γ on aqueous NH_4HSO_4, $(NH_4)_2SO_4$, and NH_4NO_3 particles.

Reference	γ	Standard error	Species [e]	RH, %	T, K
FOL03	0.01870	0.00290 [c]	1	60.1	295 [f]
FOL03	0.01860	0.00390 [c]	1	79.7	295 [f]
HAL03	0.00312	0.00167	1	20	298
HAL03	0.00407	0.00205	1	35	298
HAL03	0.03000	0.02200	1	50	263
HAL03	0.01400	0.00620	1	50	268
HAL03	0.01290	0.04500	1	50	273
HAL03	0.03630	0.01800	1	50	283
HAL03	0.01800	0.00800	1	50	298
HAL03	0.00370	0.00130	1	50	308
HAL03	0.02380	0.01200	1	70	298
HAL03	0.01560	0.00590	1	80	298
KAN01	0.00110	0.00100	1	29	295
KAN01	0.00310	0.00230	1	32	295
KAN01	0.01400	0.00520	1	34	295
KAN01	0.00320	0.00240	1	36	295
KAN01	0.00190	0.00110	1	37	295
KAN01	0.01200	0.00320	1	38	295
KAN01	0.01500	0.00130	1	43	295
KAN01	0.01800	0.00270	1	48	295
KAN01	0.01800	0.00310	1	56	295
KAN01	0.02200	0.00190	1	63	295
KAN01	0.02800	0.00290	1	67	295
KAN01	0.03500	0.01100	1	74	295
KAN01	0.06000	0.00510	1	83	295
KAN01	0.04600	0.01200	1	89	295
KAN01	0.06900	0.00950	1	99	295
MOZ88 [a]	0.05100 [b]	0.00450 [d]	1	45	274
MOZ88 [a]	0.04335 [b]	0.00300 [d]	1	45	293
MOZ88 [a]	0.08415 [b]	0.01000 [d]	1	55	274
MOZ88 [a]	0.04760 [b]	0.00500 [d]	1	55	293
MOZ88	0.06715 [b]	0.00400 [d]	1	66	274
MOZ88	0.04250 [b]	0.00350 [d]	1	66	293
MOZ88	0.08585 [b]	0.01150 [d]	1	76	274
MOZ88	0.03315 [b]	0.00600 [d]	1	76	293
BAD06	0.01500	0.00300	2	50	293 [g]
BAD06	0.01600	0.00200	2	60	293 [g]
BAD06	0.01900	0.00200	2	70	293 [g]
FOL03	0.01820	0.00320 [c]	2	62.1	295 [f]
HAL03	0.00240	0.00060	2	20	298
HAL03	0.00470	0.00130	2	35	298
HAL03	0.02500	0.00130	2	50	288

Table 1. Continued.

Reference	γ	Standard error	Species [e]	RH, %	T, K
HAL03	0.01410	0.00400	2	50	298
HAL03	0.00400	0.00800	2	50	308
HAL03	0.01490	0.00520	2	70	298
HAL03	0.01640	0.00440	2	80	298
HU97	0.04400	0.00800	2	50	297
HU97	0.05300	0.00600	2	68.5	297
HU97	0.02300	0.00400	2	83	297
HU97	0.01700	0.00200	2	93.5	297
KAN01	0.00390	0.00340	2	42	295
KAN01	0.00250	0.00120	2	45	295
KAN01	0.00410	0.00230	2	48	295
KAN01	0.01300	0.00240	2	51	295
KAN01	0.01200	0.00087	2	55	295
KAN01	0.01100	0.00110	2	58	295
KAN01	0.00600	0.00100	2	62	295
KAN01	0.01800	0.00210	2	65	295
KAN01	0.02000	0.00230	2	72	295
KAN01	0.02500	0.00096	2	76	295
KAN01	0.03300	0.00130	2	86	295
KAN01	0.04200	0.00220	2	92	295
MOZ88	0.03655 [b]	0.00250 [d]	2	60	293
FOL01	0.00415	0.00075	3	53.7	293.6
FOL01	0.00609	0.00152	3	60	297.0
FOL01	0.00959	0.00100	3	71.3	294.1
FOL01	0.01540	0.00300	3	79.6	297.6

[a] Not used in our statistical analysis based on the discussion in HAL03 (see text for details).

[b] Published γ values from MOZ88 were multiplied by 0.85 in this table based on correction factors for the plug flow approximation described by Fried et al. (1994).

[c] Average of separate standard errors reported above and below the γ value.

[d] Published values from MOZ88 are 2 times standard error. Those values are divided by 2 in this table for consistency with other papers which report 1 standard error.

[e] Species 1 = NH_4HSO_4, Species 2 = $(NH_4)_2SO_4$, and Species 3 = NH_4NO_3.

[f] Measurements were collected between 293 and 297 K. Midpoint of this range, 295 K, is used in our analysis.

[g] BAD06 does not state the temperature at which their experiments were conducted. The 293 K value is obtained from the experimental description by Badger et al. (2006b).

Table 2. Laboratory measurements of γ on dry NH_4HSO_4 and $(NH_4)_2SO_4$.

Reference	γ	Standard error	Species [e]	RH, %	T, K
KAN01	0.00150	0.00042	1	13	295
KAN01	0.00180	0.00140	1	15	295
KAN01	0.00480	0.00180	1	21	295
MOZ88 [a]	0.00510 [b]	0.00350 [c]	1	1	274
MOZ88 [a]	0.00765 [b]	0.00100 [c]	1	1	293
MOZ88 [a]	0.02040 [b]	0.00400 [c]	1	12	274
MOZ88 [a]	0.01700 [b]	0.00250 [c]	1	12	293
MOZ88 [a]	0.01870 [b]	0.00400 [c]	1	25	274
MOZ88 [a]	0.02975 [b]	0.00250 [c]	1	25	293
MOZ88 [a]	0.04675 [b]	0.00120 [c]	1	34	274
MOZ88 [a]	0.02125 [b]	0.00500 [c]	1	34	293
BAD06	0.00570	0.00060	2	25	293 [f]
HAL03	0.00170	0.00040	2	20	298
HAL03	0.00400	0.00140	2	35	298
HAL03	0.01170	0.00200 [d]	2	50	278
HAL03	0.01240 [d]	0.00220 [d]	2	50	288
HAL03	0.00460	0.00080	2	50	298
HAL03	0.00030	0.00340	2	50	308
KAN01	0.00094	0.00059	2	8	295
KAN01	0.00400	0.00096	2	32	295
KAN01	0.00380	0.00085	2	37	295
KAN01	0.00580	0.00025	2	38	295
KAN01	0.00620	0.00120	2	39	295
MOZ88 [g]	<0.00255 [b]	NA	2	25	293

[a] Not used in our statistical analysis based on the discussion in MOZ88 (see text for details).

[b] Published γ values from MOZ88 were multiplied by 0.85 in this table based on correction factors for the plug flow approximation described by Fried et al. (1994).

[c] Published values from MOZ88 are 2 times standard error. Those values are divided by 2 in this table for consistency with other papers which report 1 standard error.

[d] Table 4 in HAL03 contains typographical errors. Corrected values appear in this table based on personal communication with R. A. Cox.

[e] Species 1 = NH_4HSO_4 and Species 2 = $(NH_4)_2SO_4$.

[f] BAD06 does not state the temperature at which their experiments were conducted. The 293 K value is obtained from the experimental description by Badger et al. (2006b).

[g] These data were not used in our analysis due to the missing standard error and uncertain γ value.

Table 3. Regression coefficients and summary statistics for Eqs. (4–6) and (9).

(a) Summary statistics for the aqueous NH_4HSO_4 and $(NH_4)_2SO_4$ model (i.e., λ_1 and λ_2).

	Estimate	Std Error	t value	p value
β_{10}	−4.559088	0.212216	−21.483	<2e-16
β_{20}	−0.369769	0.100070	−3.695	0.000508
β_{11}	0.028593	0.003074	9.300	7.02e-13
β_{12}	−0.111201	0.016155	−6.883	5.86e-09

Multiple R-squared: 0.6808, Adjusted R-squared: 0.6634

(b) Summary statistics for the aqueous NH_4NO_3 model (i.e., λ_3).

	Estimate	Std. Error	t value	p value
β_{30}	−8.107744	0.199409	−40.66	0.000604
β_{31}	0.049017	0.002901	16.89	0.003485

Multiple R-Squared: 0.993, Adjusted R-squared: 0.9896

(c) Summary statistics for the dry NH_4HSO_4 and $(NH_4)_2SO_4$ model (i.e., λ_d).

	Estimate	Std. Error	t value	p value
β_{d0}	−6.133764	0.165600	−37.040	9.62e-14
β_{d1}	0.035920	0.004328	8.300	2.57e-06
β_{d2}	−0.196879	0.028148	−6.994	1.45e-05

Multiple R-Squared: 0.8991, Adjusted R-squared: 0.8823

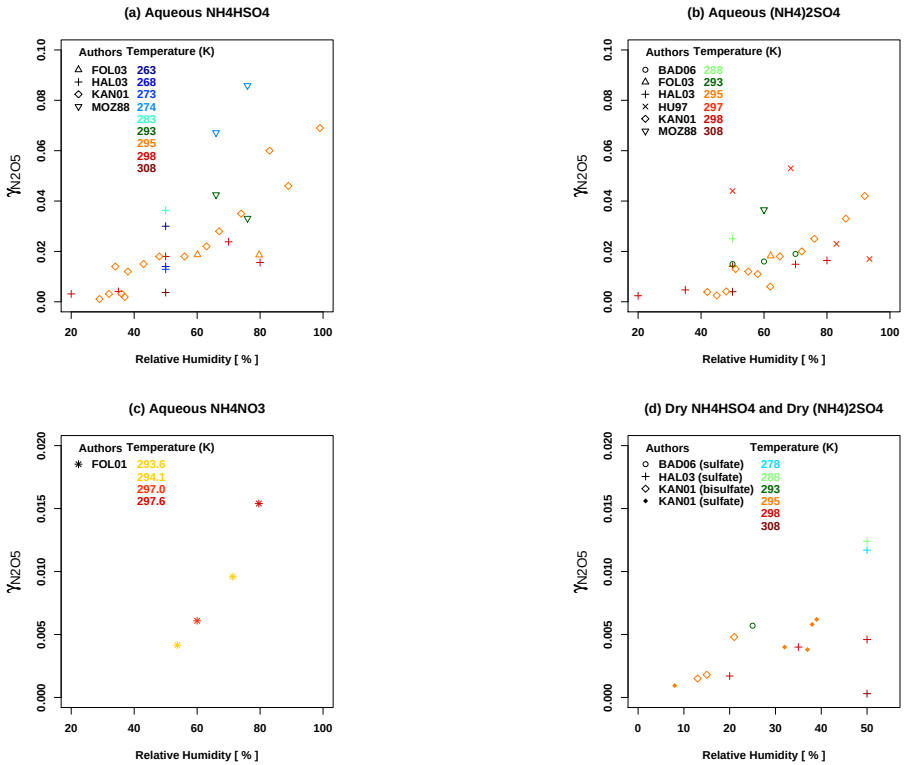

Fig. 1. Laboratory measurements of γ used in the statistical models for **(a)** aqueous NH_4HSO_4, **(b)** aqueous $(NH_4)_2SO_4$, **(c)** aqueous NH_4NO_3, and **(d)** dry NH4HSO4 and $(NH_4)_2SO_4$.

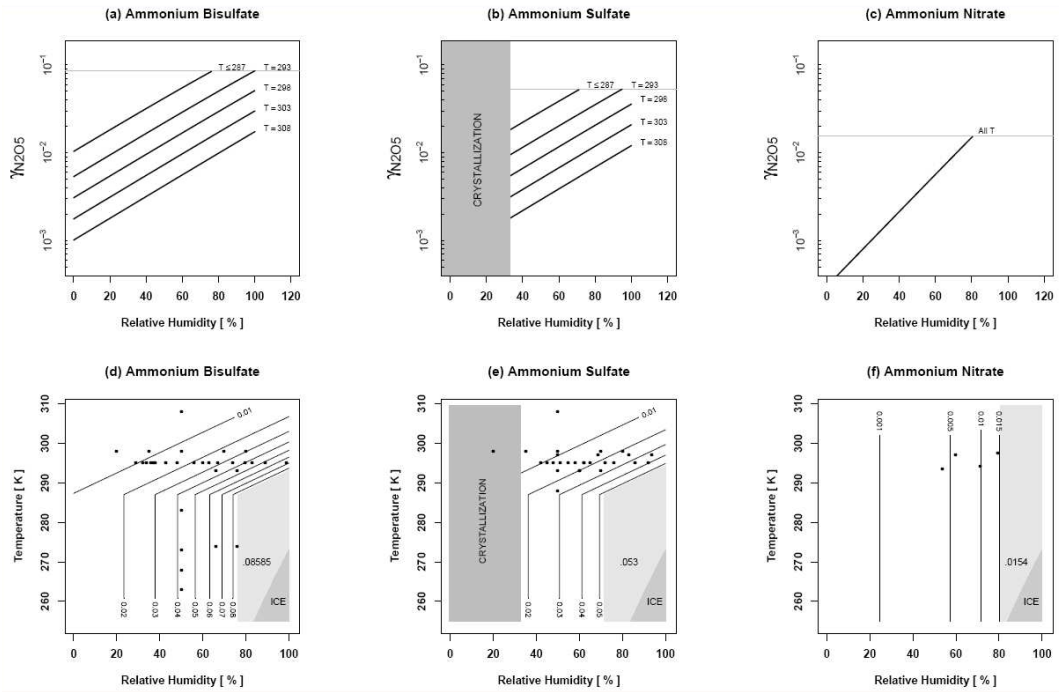

Fig. 2. Parameterization of γ as a function of RH and T for (**a** and **d**) aqueous NH_4HSO_4, (**b** and **e**) aqueous $(NH_4)_2SO_4$, and (**c** and **f**) aqueous NH4NO3. In (d–f), contour lines show the parameterized value of γ and discrete points show the combinations of T and RH at which laboratory measurements were collected. Shaded regions are described in the text.

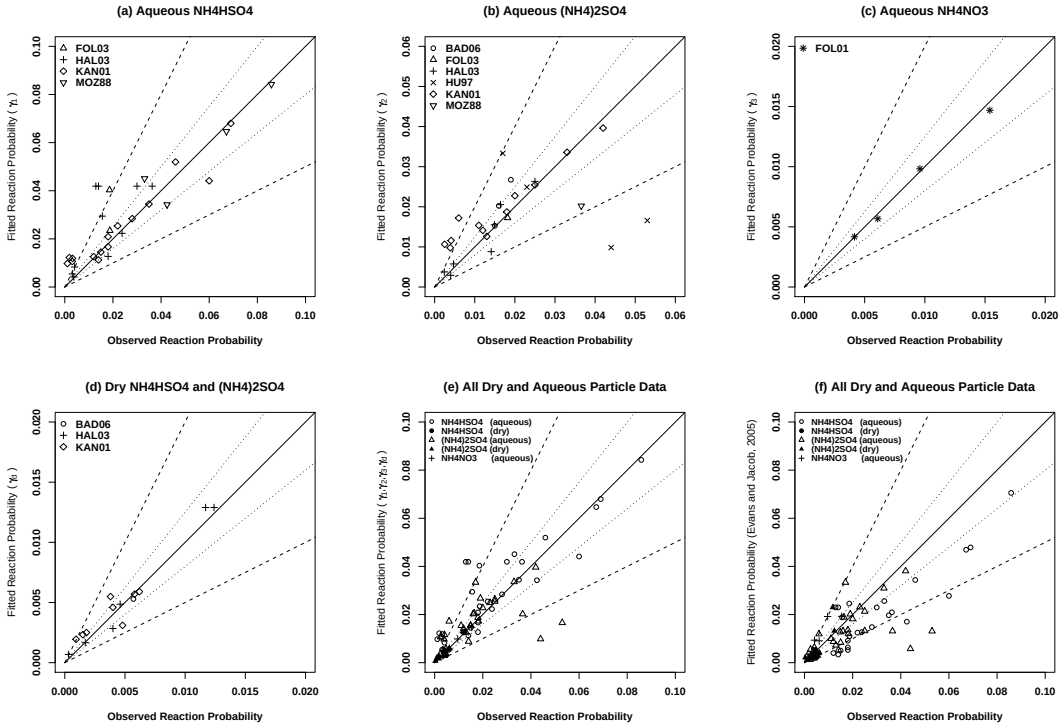

Fig. 3. Comparison between the parameterized and observed γ values using (**a–e**) our regression equations and **(f)** the Evans and Jacob (2005) parameterization for sulfate particles. Dashed and dotted lines bound the data points which are fit within factors of 2 and 1.25, respectively. Solid lines depict 1:1 agreement.

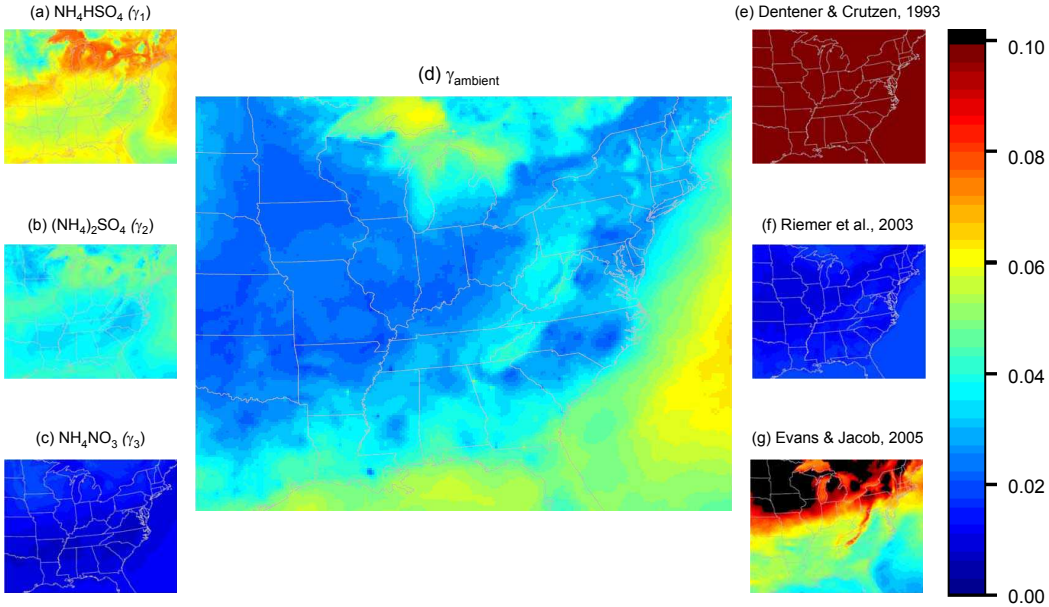

Fig. 4. Average nighttime values of γ over the eastern United States during January-February 2001, comparing **(a–d)** our parameterizations with **(e–g)** those used in previous model applications. In (a, c, and g), γ is a function of RH and T. In (b), γ is a function of RH, T, and phase state. In (e), γ is fixed at 0.1. In (f), γ is a function of SO_4^{2-} and NO_3^-. In (d), γ is a function of RH, T, SO_4^{2-}, NH_4^+, NO_3^-, and phase state. All γ values greater than 0.1 are plotted in black.